RADIALLY-SYMMETRIC SILICONE BELLOW SOFT ACTUATORS FOR A ROBOTIC REHABILITATION EXOGLOVE

Thesis

Submitted in Partial Fulfillment of

the Requirements for

the Degree of

MASTER OF SCIENCE (Mechatronics and Robotics)

at the

NEW YORK UNIVERSITY

TANDON SCHOOL OF ENGINEERING

by

Arunagiri Adhithian Ravichandran

May 2023

RADIALLY-SYMMETRIC SILICONE BELLOW SOFT ACTUATORS FOR A ROBOTIC REHABILITATION EXOGLOVE

Thesis

Submitted in Partial Fulfillment of
the Requirements for
the Degree of

MASTER OF SCIENCE (Mechatronics and Robotics)

at the

NEW YORK UNIVERSITY

TANDON SCHOOL OF ENGINEERING

by

Arunagiri Adhithian Ravichandran

May 2023

Approved:

____

Advisor Signature

____

Date

____

Department Chair Signature

____

Date

University ID: N10046805
Net ID: ar7404

VITA

Arunagiri Adhithian Ravichandran was born in Chennai, India on October 13th, 1998. He has a bachelor's degree in Mechanical Engineering acquired from Anna University, during which he has published papers on the vibrational analysis of natural fibers. After graduating he worked in the mechanical industry specializing in molding technologies for a year. After this, he got admitted into NYU Tandon School of Engineering to pursue his Master of Science in Mechatronics and Robotics Engineering, where he worked at MERIIT (Medical Robotics and Interactive Intelligent Technologies) laboratory during which his study on soft robotic actuators for rehabilitation was researched on.

ACKNOWLEDGEMENTS

I would like to thank my thesis advisor, Professor Farokh Atashzar of the School of Engineering at New York University, for his constant guidance and encouragement. Thank you for the great learning opportunity that you have given me during my thesis.

Next, I would like to thank my thesis mentor, Dr. Jacqueline Libby, for always helping and steering me in the right direction whenever needed as well as putting such time and effort into my thesis research that helped me achieve all the success. I would like to thank her for teaching me to work with various research methods that would be helpful to me throughout my career.

I would also like to thank all my fellow researchers at MERIIT lab for their unceasing support and aid throughout the research.

Finally, I am grateful to my parents and family for providing me with unfailing support in all my decisions, and continuous encouragement throughout my years as a master's student at New York University. This accomplishment would be impossible without them. Thank you.

ABSTRACT

RADIALLY-SYMMETRIC SILICONE BELLOW SOFT ACTUATORS FOR A ROBOTIC REHABILITATION EXOGLOVE

by

Arunagiri Adhithian Ravichandran

Advisor: Prof. Farokh Atashzar

Submitted in Partial Fulfillment of the Requirements for

the Degree of MASTER OF SCIENCE (Mechatronics and Robotics)

May 2023

Soft robots have attracted significant attention in recent years due to their inherent compliance. Inspired by bionics, soft robots generate motion and force with compliance that mimics the softness of the human body, allowing them to be safer for physical Human-Robot Interaction (pHRI). The development of soft actuators is still in its early stages, both in design and control. This thesis pushes the envelope in the design of soft actuators and soft robots, presenting a sophisticated bellow soft actuator as a component within an assembled exoglove. The presented soft actuator is a miniaturized, radially-symmetric bellow design, which is highly compliant and capable of both positive and negative actuation. The bellow body is assembled into a hybrid soft-hard modular component, and these modules are assembled onto an exoglove. This thesis presents the full fabrication pipeline to actualize this design, including 3D printing of mold and hybrid components, improved lost-wax casting, injection molding, hybrid soft-hard assembly of each modular actuator, and assembly of the modules into a conceptual glove design. The glove is presented as a proof-of-concept for future rehabilitation and assistance applications in the medical domain, such as for tetraplegic individuals or patients post-surgery. The experimentation and results of this thesis pave the way to develop more advanced soft robots having intricate features.

TABLE OF CONTENTS

LIST OF FIGURES

Chapter 1

1. Introduction

1.1 Motivation

The advancement of rehabilitation technologies [1] in the past decade has created a specific interest in the use of silicone actuators in soft robotic hand rehabilitation devices since these are extremely easy to manufacture and can create a curved motion for a simplified input. One of the most complex biomechanical systems [2] present in the human body is the human hands, making it one of the most interesting and challenging topics for rehabilitation.

Rehabilitation therapy is a form of treatment that helps individuals recover from physical or mental disabilities, injuries, or illnesses. In order to achieve the best possible outcome, it is crucial to tailor the therapy to the specific needs of the patient. The important factor is to maintain precise control over the force, frequency, and position of the treatment. Force refers to the amount of pressure applied, frequency refers to the number of times the therapy is administered within a certain time frame and position refers to the placement of the patient's body during therapy. The quality of rehabilitation by using the above criteria for the hand's biomechanical system can only be provided using a robotic glove. By using a robotic glove, the need for a therapist is also excluded making the process easier to be performed at home [3].

At present, there are two main types of robotic glove devices for hand rehabilitation: rigid and soft exoskeletal gloves [4]. Rigid actuators consist of rigid parts such as hinges, motors, etc. which may cause harm to the patient if not actuated properly or if any error occurs because these types of actuators are more rigid than the human hand. Thus, soft actuators are the only viable option to be used [5]. In order to assist all the joints, present in the hand's biomechanical system, the most practical solution requires a micro-scaled actuator. A previous study [6] shows that pneumatic actuators can provide the highest force, reliability, and power when micro-scaled. Another crucial advantage of using a pneumatic actuator in a rehabilitation device is that it can produce positive-negative pressure which provides both flexion and extension motion of the fingers, which is crucial in treating cumulative trauma disorders like spasticity, arthritis, etc.,

1.2 Previous works

In 2013, a soft robotic glove [7-8] was designed by Panagiotis Polygerinos to aid the rehabilitation of individuals with grasp pathologies which included the study of the design and creation of the actuator and a preliminary assessment of the actuator's effectiveness. Even though Polygerino's glove design addressed many issues, it has some drawbacks such as:

- The actuator acts as an elastic return which is being provided for the retraction motion of the fingers, which mimics the behavior of the negative pressure but is not effective over a period because the elasticity degrades over a period of usage due to micro tears.
- Since the elasticity of the material cannot be controlled, it causes the retraction behavior to be customized with respect to any metrics such as force, frequency, etc. There is also no data set on how to choose a specific material to meet certain conditions.
- On top of all the drawbacks, the aforementioned robotic glove fails to provide thumb adduction and abduction which is required to rehabilitate thumb surgeries such as thumb trigger release.

Figure 1 Soft robotic glove by Panagiotis Polygerinos [2015]

In 2020, a soft robotic glove [9] was developed by Debin Hu that uses a positive-negative pneumatic actuator made of symmetrical bellows that have been experimentally measured and the force along the axis of actuation has been analyzed. The glove design can provide adduction and abduction of the thumb finger by placing an actuator in the purlicue region. The two types of actuators designed in this work have been set to have a diameter of 16 mm to fit the width of the finger and the lengths are set to 24mm and 32mm for the IP joints and MP joints of the hand respectively. Even though many issues have been addressed in this work, the presented glove fails to address some key issues:

- The actuator bulges away from the dorsal face of the hand during actuation.
- This work does not present the material or the fabrication process that has been implemented in order to fabricate the miniaturized actuator that has been used in the robotic glove.

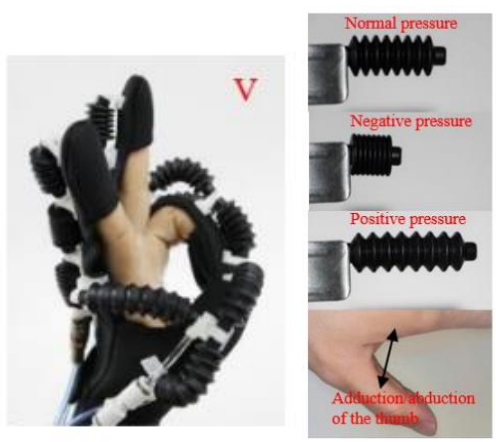

Figure 2 Soft robotic glove (left) with PNP actuator (right)

Many studies have been conducted in the past in the field of microactuators and hybrid actuators that have significantly contributed to this research. Below this is a brief overview of some of the most important findings.

Soft actuators have been made to mimic animal characteristics. A study was carried out in 2017 [10] where a novel robust hybrid bending actuator for a rehabilitation glove was fabricated by reinforcing both rigid and soft components inspired by crustaceans.

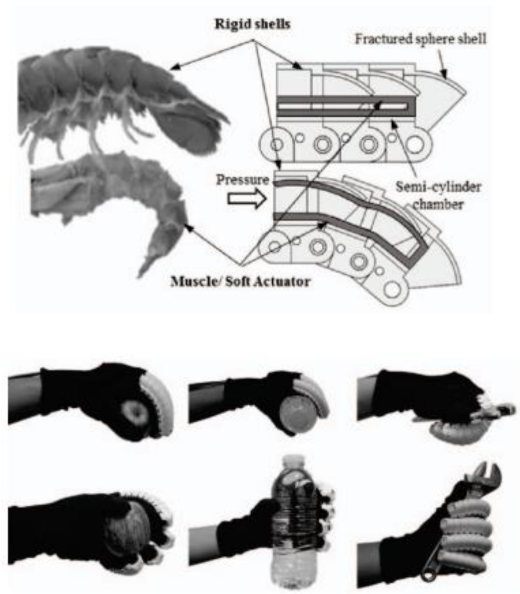

Figure 3 Lobster-inspired actuator mechanism (top) along with manipulation tasks (bottom)

In 2018, a soft robotic glove [11] was developed by reinforcement of elastomer two thermoplastic elastomer balloons with one stretchable upper layer and two inextensible bottom layers. The upper chamber during inflation results in flexion and the lower chamber exhibits extension during inflation. This study analyzes the mechanical characteristics of the actuator and the different configurations of inextensible fabric in order to get customized functionality.

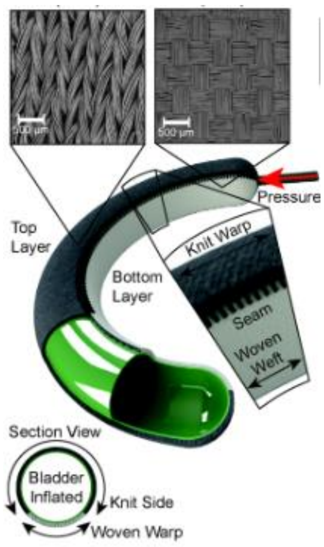

Figure 4 Balloon elastomer actuator sectional view

Recently in 2022, a study [12] was conducted that describes the design and fabrication of a soft actuator that utilizes a symmetrical bellow structure and employs an improved casting method [13] by using paraffin wax. The soft actuator's performance was evaluated by constructing an experimental platform to test its deformation under varying pressure.

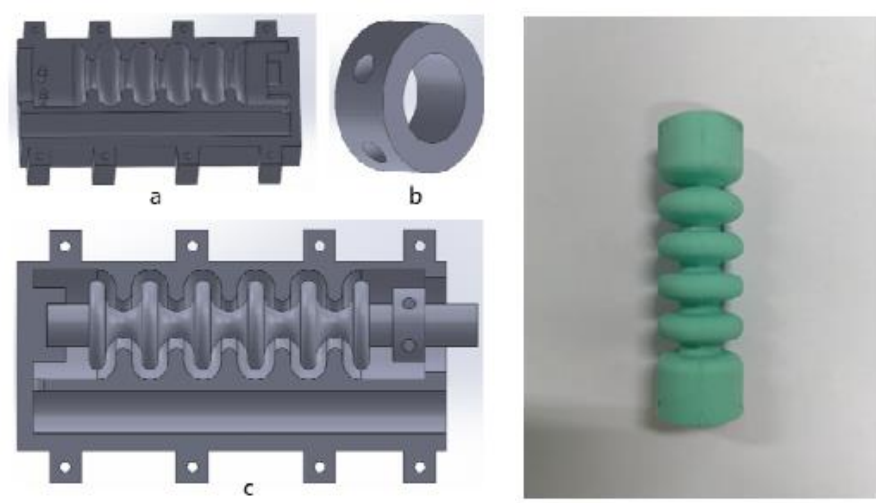

Figure 5 The mold (left) for making the silicone actuator (right)

1.3 Goal

The goal of this study is to present a novel radially-symmetrical bellow-shaped soft actuator fabricated through the process of injection molding and 3D-printed inextensible reinforcement parts in order to overcome the aforementioned drawbacks and possibly create a glove for hand rehabilitation. We will be using an inner wax core fabricated using a casting method to create the inner bellow shape of the actuator so that the core can be easily removed after fabricating the thin-walled bellow actuator. We will be using Sorta Clear – 40 silicone mixture which has a soft consistency that allows for rapid actuation at various frequencies.

1.4 Thesis outline

This thesis presents a comprehensive manufacturing process of a soft bellow type actuator, accompanied by various design options aimed at incorporating the reinforcement features to meet specific requirements.

In Chapter 1, the motivation for this research along with the various previous works done related to this research and the goal of this research has been defined.

In Chapter 2, the design and fabrication of the actuator along with its iterations have been discussed. The fabrication of the inner core and outer silicone layer has also been defined along with its iterations. The design and fabrication of the reinforcement layers along with their iterations have also been discussed.

In Chapter 3, the experimental setup and different types of reinforcement along with its behavior will be discussed in the result.

In Chapter 4, the concluding remarks of this thesis have been put forward along with the possible ways of future work.

Chapter 2

2 Methodology

In this chapter, the fabrication process of the soft silicone actuator and the iterations done during the development are explained. The soft reinforcement actuator is fabricated in four stages. The first stage requires fabricating the inner wax core. The second stage is degassing and injection molding of silicone. The third stage is the process where the inner core is melted and cleaned. The fourth stage involves designing and manufacturing reinforcement parts.

2.1 Inner wax core

To fabricate the inner core a wax mold is constructed with 4 parts assembled. The mold is designed this way, so that alignment of parts of the mold is obtained while assembling. This alignment gives the ability to fabricate an inner core with accurate dimensions. The parts of the mold are 3D printed in PLA (Polylactic Acid) using Ultimaker S3 at high precision with a 0.4mm nozzle and a layer height of 0.2mm. To obtain higher accuracy in the detail of the mold the print speed was set to 30 mm/s and infill density was set to 30% to reduce the print time. The parts are designed in a way that does not require any support material while printing, which makes the process of cleaning the molds easier. Adhesion is required to be printed along for the part to be removed without any damage. After the printing, the adhesion layer is removed using a clipper, and the edges are sanded down so that the parts sit on each other with perfect alignment. The parts are assembled using m4 screws and nuts as shown in Fig 6.

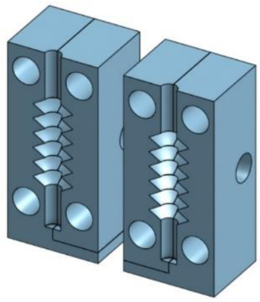

Figure 6 3D CAD model of the wax mold

After assembling the mold, the beeswax is melted in a beaker at 250 F. Once the beeswax is completely in a liquid state, the beaker is removed from the heat and air-cooled until the liquid reaches 177 F without solidifying. The temperature was identified to be 177 F after various trials and errors. Because if the temperature was below 177 F the inner wax core had blunt edges as you can see from Fig 7.

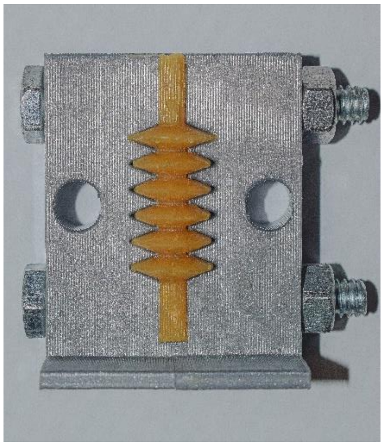

Figure 7 Wax inner core with blunt edges.

If the temperature was higher than 177 F the inner core gets stuck to the mold and gets damaged while trying to remove it from within the mold. Once the liquid reaches 177 F the mold is filled by using a continuous pour. The mold is then left to cure for 24 hours in atmospheric air and temperature. After curing the mold is demolded by carefully removing one part of the assembled mold at a time to obtain the wax core shown in Fig 8.

Figure 8 Wax inner core with sharp edges.

2.2 Silicone actuator

In the second stage injection molding is used to fabricate the required silicone-based soft bellow actuator. To fabricate the required actuator, the mold in 3D printed into two parts as shown in Fig 9.

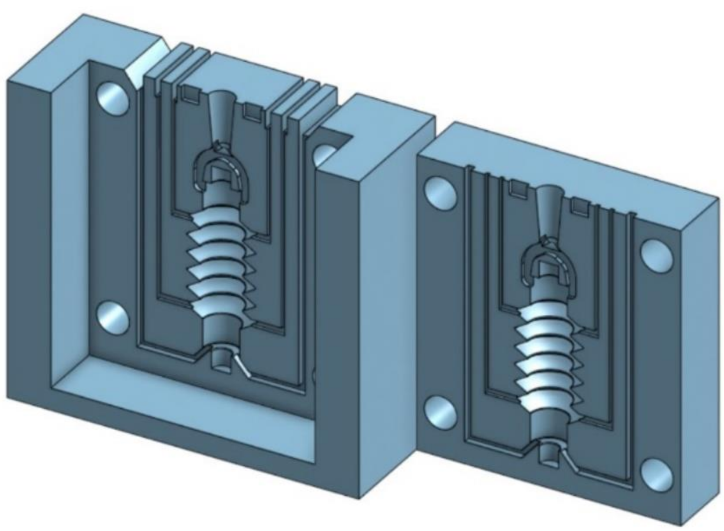

Figure 9 3D CAD model of the silicone mold

The parts are printed in PLA (Polylactic Acid) using Ultimaker S3 at high precision using a 0.4mm nozzle and with a layer height of 0.2mm. To obtain a higher definition of the mold the 3D printer was configured to run at a slow speed of 30mm/s and the infill density used was 30% to reduce the print time. The parts are designed in a way that does not require any support material while printing, which makes the process of cleaning the molds easier. Adhesion is required to be printed along for the part to be removed without any damage.

After the printing, the adhesion layer is removed using a clipper, and the edges are sanded down so that the parts sit on each other with perfect alignment. Then the wax core is placed inside the mold as shown in Fig 10 and assembled using an m4 screw and nuts.

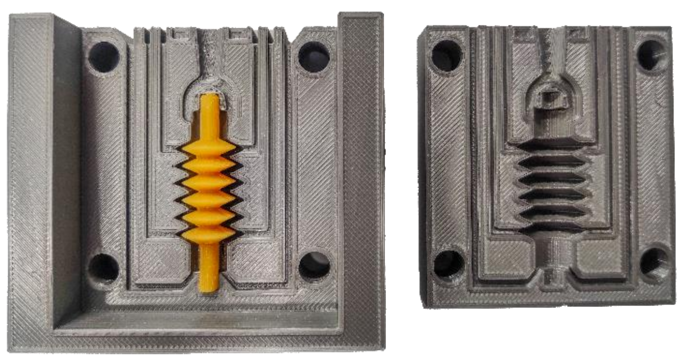

Figure 10 Wax inner core placed inside the silicone mold.

The silicone mixture used to fabricate the soft bellow actuator here is Sorta Clear – 40. We are using a softer silicone material than other rubbers to increase the frequency of actuation. From the datasheet, the pot life of this mixture is 40 minutes and the curing time that it would require is 16 hours at atmospheric temperature. To create the silicone mixture Part-A and Part-B constituent parts of the mixture are required. 40 ml of part-A is poured into a beaker using a popsicle stick and mixed well to increase the viscosity of the material. 4 drops of violet-colored silicone rubber pigment considering 1 drop for every 10 ml of part -A is added to part – A and mixed until the pigment is evenly spread across. After adding the pigment, the beaker with part – A is weighed, and the weight is measured. After measuring the weight of part – A, an empty beaker is taken and placed on the scale for part – B to be poured in. Part – B is poured in the ratio of one-tenth of the weight of part – A to get an excellent bonding ratio. Finally, both parts are mixed until the viscosity of the mixture is the same throughout and no residual liquid of both parts is left separately within the beaker.

After mixing thoroughly, the mixture is poured into a container with a higher surface area, so that the air rises in the form of bubbles easily from within the mixture during degassing. The container is placed inside a vacuum chamber and degassed using a vacuum pump at - 0.9 psi. After degassing the mixture is poured into a 12 ml syringe by using a continuous pour, which helps in preventing air bubbles from forming. The mixture is then injected into the mold using the passageway for the syringe at the top of the mold until the mixture overflows from all six air passageways. Then the mold is left to cure for 16 hours.

2.3 Demolding

The third stage involves removing the inner wax core and cleaning the actuator of residual materials. After curing the silicone mold is demolded and the silicone actuator with inner core and excess material is taken out.

The excess material is trimmed using a clipper, and the actuator after trimming is shown in Fig 11.

Figure 11 Actuator with inner core after demolding

The actuator is held using a thong and a heat gun at 460 F is used to melt the wax from the inner part of the actuator. The melted wax is collected in a cup.

After melting the inner wax from within the actuator, the actuator is subjected to two hot water baths in a beaker to remove any residual particles of unmelted wax along the inner walls of the actuator. After the water bath, the actuator is dried at atmospheric temperature until all water on the inside of the actuator has evaporated. Fig 12 represents the actuator after removing the inner wax core.

Figure 12 Silicone actuator after cleaning

2.4 Reinforcement Parts

This fourth stage consists of manufacturing reinforcement parts to integrate them into the actuator for specific functionality. For the pneumatic air to travel between the actuators and to prevent the pneumatic air from escaping from the end actuator, connectors, and blockers are 3D printed in PLA using Ultimaker S3 at a reduced speed of 30mm/s. Fig 13 shows the pictorial representation of the connectors and the blockers. The longer connector is designed to connect the actuator between MP joints and the smaller connector is used to connect IP joint actuator. The cylindrical poles on the flat surface are used to fix the limiting layer and ridges along the circumference prevent the zip tag from moving to hold the actuator.

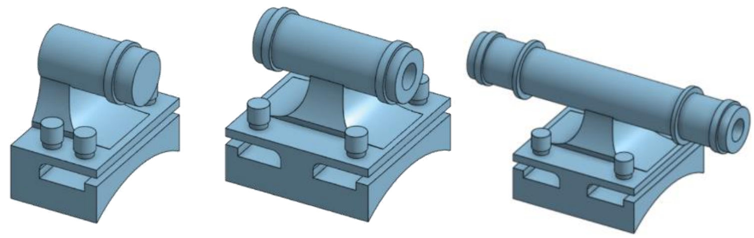

Figure 13 3D CAD model of Blocker (left), Connector IP joint (Middle), Connector MP joint (Right)

Limiting layers and rings, shown in Fig 14 and Fig 15 are 3D printed in TPU (Thermoplastic polyurethane) using Ultimaker S3 a thickness of 0.75 mm. The holes in limiting layers are attached to the poles of the connectors or blockers to prevent the actuator from translating in a line and to convert the motion of the actuator into a curved path. The limiting rings prevent the actuator from expanding radially and at the same time increase the pneumatic pressure along the access of the actuator. Rings with feet prevent radial expansion and bulging of the actuator.

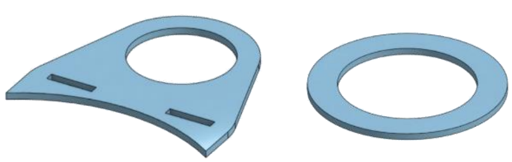

Figure 14 Rings with feet and without feet

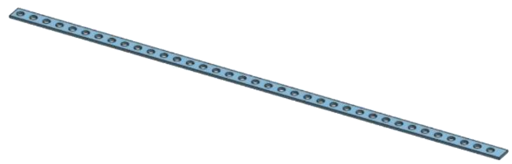

Figure 15 Limiting layer.

2.5 Assembled Actuator

The proposed actuator in this research is assembled as follows, the rings are slid into the valleys of the actuator first. The connectors and blockers are slid into the actuator's sleeves until it is completely in. The ridges on the connectors help zip-tag the actuators to the connectors or blockers. The zip tags help prevent air from leaking from the actuator. Limiting layers are then attached to the poles of the connectors or blockers based on the joint length and superglued. Fig 16 represents the assembled actuator.

Figure 16 Assembled Actuator with rings with feet.

2.6 Actuator Dimensions

Based on the design of Debin Hu's actuator, the actuator was designed to have a symmetrical bellow on both sides. The length of the actuator was set to 38 mm for the DIP and PIP joints of the hand. For the MCP joints, a longer actuator was manufactured with a 58 mm overall length having ten air chambers. The thickness of the actuator at the peaks and valleys was set to 2.5 mm while designing without 0.15 mm chamfer at the outer peak and valley. Fig 17 shows the dimensions using the sectional view.

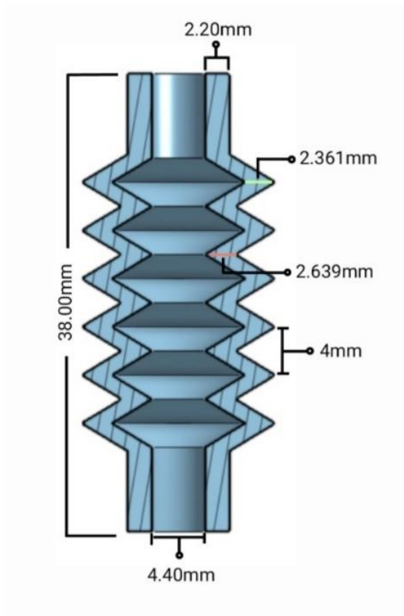

Figure 17 Actuator (DIP and PIP joints) dimensions

2.7 Mold Improvements

The wax mold was perfected in two iterations. The first iteration [14] using Ultimaker S3 shown in Fig 18 was 3D printed in PLA. As you can see from the figure it can be seen that the mold was fabricated in 4 parts. From the figure, it can be seen that there is no alignment mechanism used in the first iteration.

Since the mold is being assembled by human hands the alignment of the molds varies from pour to pour. This phenomenon causes the inner wax core to be manufactured with improper dimensions during wax pouring which in turn changes the inner design of the soft actuator.

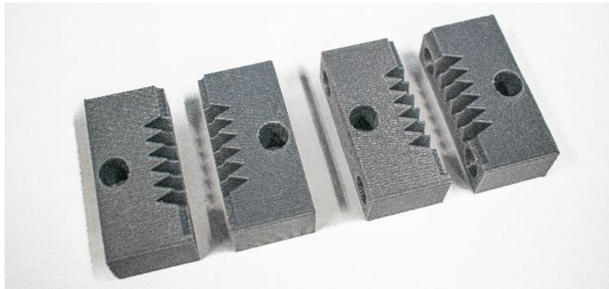

Figure 18 Wax mold first iteration

To remove this error of misalignment the parts of the mold were designed as shown in Fig 19. By making two parts alternate parts identical to each other, one part can sit on the other to create a near-perfect alignment. This design approach gives us the benefit of creating a wax core that has accurate dimensions to it.

Figure 19 Wax mold second iteration

The silicone mold was perfected in two iterations. The first iteration shown in Fig 20 was printed Ultimaker S3 in PLA. As you can see from the figure, the two parts of the mold are identical to each other. The problems with this mold are that there is no alignment between the parts. Since the mold is being assembled by human hands the alignment of the molds varies from pour to pour. This phenomenon causes the outer silicone layer manufactured be with improper dimensions. Another problem that was noticed during the fabrication process was that, since all the air passageways are at the same height, the last air passageway gets filled first because of the pressure from the syringe. This causes the excess material from the furthest air passage to cover on top of other passages ways causing air to be trapped within the air passageways. This trapped air sometimes causes holes to be formed in the silicone layer causing air leakages. The third problem was the anchor on which the wax core will be placed. Since the anchor was 0.25mm and 1.75mm the wax core did not have a firm hold to maintain its position once the mold is tightened. This caused movement of the inner core inside the outer mold.

Figure 20 Silicone mold first iteration

In the second iteration as shown in Fig 21 the alignment issue was solved by having three sided guide on one part of the mold, within which the other part will be fitted in with alignment. This design process helped in acquiring silicone actuators with accurate dimensions.

To solve the overflowing problem, overflow channels were designed so that the excess material flowing out of the passageway is redirected to flow away from the other passageways. The anchor problem was solved by increasing the length of the anchor to 4mm on either side so that there is a firm hold on the inner wax core.

Figure 21 Silicone mold second iteration

2.8 Process Improvements

The degassing method was improved from the traditional method of degassing. In the traditional method, once the mixture is placed inside the vacuum chamber for degassing the pump is maintained at a certain psi until the air is extracted from the mixture. But in the case of Sorta Clear – 40A, the mixture has high levels of viscosity which makes it difficult for the air to flow from inside the mixture into the vacuum.

In the first iteration of degassing, the mixture was degassed multiple times before solidification. In between each degassing, the mixture was disturbed using a popsicle stick by mixing the mixture in an ”S” pattern so that the air below the upper surface of the mixture rises which can be removed from the mixture during the next degassing. This process was repeated until all bubbles were removed from the mixture. Even though bubbles were removed from the mixture, this process took about 40 – 45 minutes. Considering the pot life of the mixture is 60 minutes after 40 - 45 minutes the flowability of the mixture reduces drastically which makes it difficult to be poured inside the syringe to be injected.

To tackle the time constraint problem in the first iteration of degassing, the method of abruptly injecting air into the vacuum chamber was required. To elaborate on the previous statement, once the mixture is placed into the vacuum chamber, the pressure is maintained to be -0.9 psi until all air rises as bubbles to the top surface of the mixture until it reaches the state of bursting. Now, the inlet air valve is opened abruptly causing the bubble to burst. After the vacuum chamber is at atmospheric pressure, degassing is started again and the process mentioned above is repeated until the mixture is completely degassed. This method of degassing reduced the time required from 40 - 45 minutes to 20 – 25 minutes and the flowability of the mixture was improved.

2.9 Actuator dimension improvements

The first iteration [15] of the actuator had numerous errors in it. Fig 22 represents the sectional view of the CAD model of the actuator. As you can see the thickness at peaks at the air chamber is 1.351mm and the thickness at the valleys of the actuator is 2.999mm. This difference in thickness has caused the walls of the actuator to be non–parallel. The minimum thickness along the wall was 0.752mm. This thickness alone was too small to be created without any tears forming in it. This caused some actuators that were fabricated to have a tear in them causing air leakage. The sleeve length was also varied on both sides of the actuator.

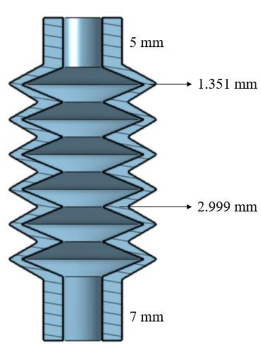

Figure 22 Actuator first iteration

In the second iteration, as shown in the sectional view in Fig 23, the thickness of the actuator at peaks and valleys was set to a constant of 1.5mm. The difference in thickness at peaks at valleys even though the thickness was set to constant is due to the chamfering of 0.15mm on the outside peaks and outside valleys. As you can see now the actuator walls are parallel giving us a constant wall thickness of 0.540mm. Since this is less than the thickness of the first iteration, this actuator design will not be suitable for fabrication as it tore easily while demolding. The sleeve length was also made constant to 5mm on both sides. But 5mm sleeve length was not enough for the zip tag to sit on and prevent the actuator from loosening.

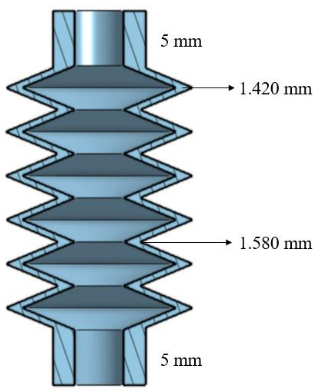

Figure 23 Actuator second iteration

In the third iteration, as shown in the sectional view in Fig 24, the thickness of the actuator at peaks and valleys was set to a constant of 2mm. The difference in thickness at peaks at valleys even though the thickness was set to constant is due to the chamfering of 0.15mm on the outside peaks and outside valleys. As you can see, now the actuator walls are parallel giving us a constant wall thickness of 0.830mm. Even though this thickness was suitable for fabrication it caused tears as shown in Fig 24 The sleeve length was also made constant to 7mm on both sides so that the zip tags can be tied onto the blocker or connector.

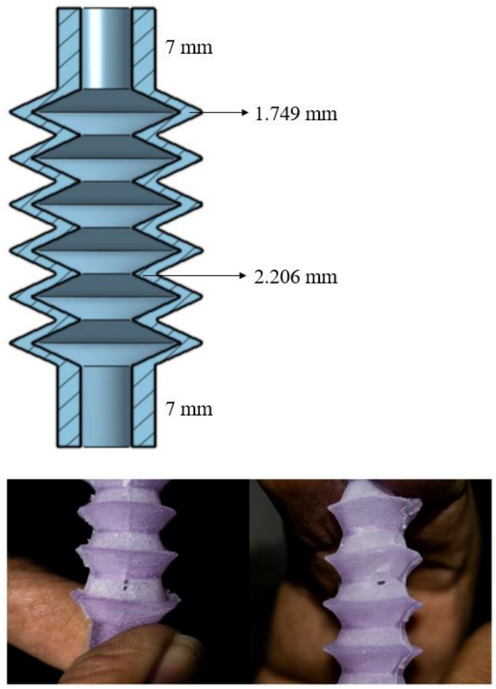

Figure 24 Actuator Third Iteration (top), Corresponding actuator with tears (bottom)

In the fourth iteration as shown in the sectional view in Fig 25 the thickness of the actuator at peaks and valleys was set to a constant of 2.5mm. The difference in thickness at peaks at valleys even though the thickness was set to constant is due to the chamfering of 0.15mm on the outside peaks and outside valleys. As you can see, now the actuator walls are parallel giving us a constant wall thickness of 1.296mm. Using these dimensions, the actuator can be fabricated with the least defects as the success rate was 90% based on the fabrication of 10 actuators.

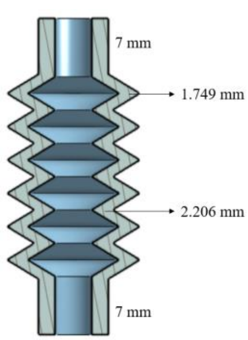

Figure 25 Actuator fourth Iteration

2.10 Glove design and fabrication

The glove is fabricated by integrating a soft knit glove (manufactured by Achiou made with an outer layer made up of 86% acrylic, 13% polyester, and 1% spandex and an inner layer made up of 100% polyester) with foam to reduce elasticity at required places. Fig 26 shows the schematic drawing of the assembly of the glove.

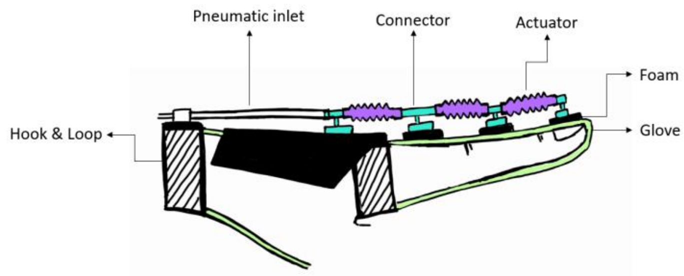

Figure 26 Schematic diagram of the glove (side)

There are large foam pieces attached on the dorsal side of the hand and the wrist using super glue to prevent the actuator from lifting from the dorsal side of the hand and for pneumatic tubes to place along the wrist. There are hook and loop straps on the palm side of the hand and the wrist. The hook and loop strap on the palm increases the tightness of the glove to the hand. The hook and loop straps along the wrist prevent the glove from slipping away from the hand.

This type of integration makes the glove design simple and easier to be worn by patients post-surgery. Fig 27 shows the glove. Fig 28 shows an actuator integrated at the DIP joint of the index finger.

The foam is placed for the entire length in between the joint so that actuator can be placed at any point on the finger based on the subject's hand.

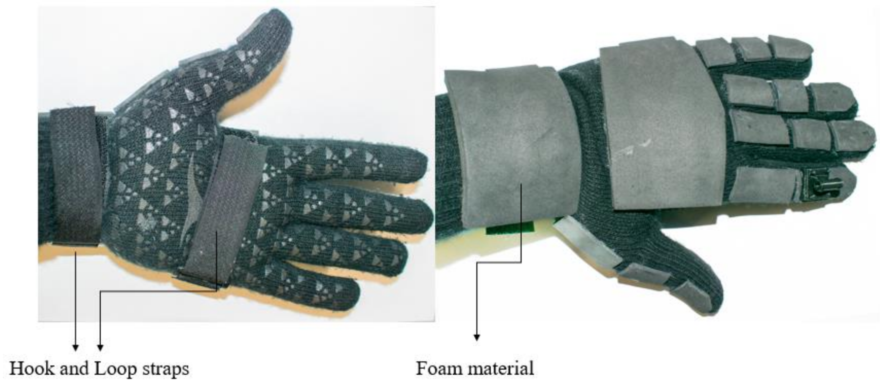

Figure 27 Glove palm side (left) Glove dorsal side (right)

Figure 28 Glove with actuator integrated at the index finger

Chapter 3

3 Experimentation and Validation

3.1 Experimental setup

To test and study the fabricated actuator, an experimental setup was created by plugging a plastic tube into a large syringe. The syringe was marked with labels to set limits to the pressure that the actuator can manage. Using the connector, the free end of the plastic tube was connected to the actuator. Fig 29 depicts the experimental setup.

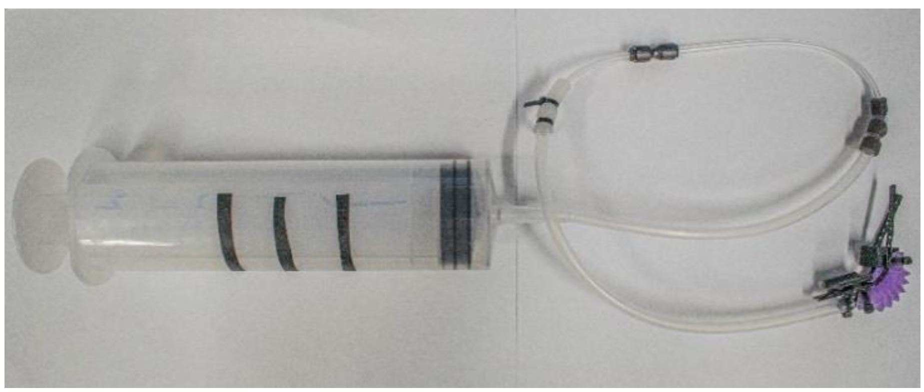

Figure 29 Experimental setup with a syringe

3.2 Actuator with limiting layer

The actuator was connected to the syringe using a connector and a blocker was affixed to the other end. The actuator was reinforced with just the limiting layer as shown in Fig 30 to observe how the actuator acted and the results were recorded.

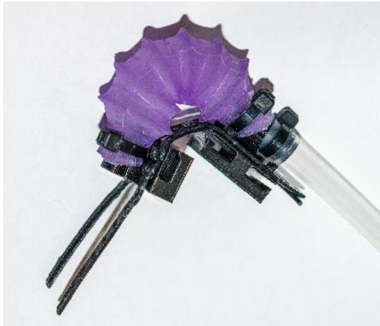

Figure 30 Actuator with just limiting layer

3.3 Actuator threaded

The actuator was connected to the syringe using a connector and a blocker was affixed to the other end. The actuator was reinforced with threads at valleys as shown in Fig 31. Each valley has 6 rounds of thread wound around it. The responsiveness of the actuator was observed and recorded.

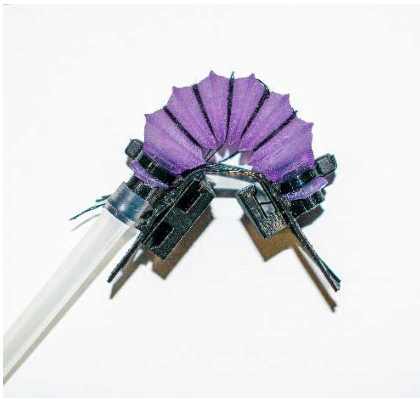

Figure 31 Actuator threaded.

3.4 Actuator reinforced with rings

The actuator was connected to the syringe using a connector and a blocker was affixed to the other end. The actuator was reinforced with rings without feet at valleys as shown in Fig 32. The responsiveness of the actuator was observed and recorded.

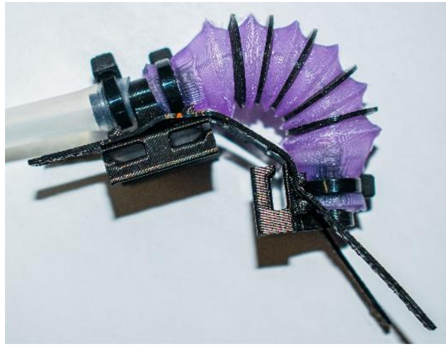

Figure 32 Actuator with rings

3.5 Actuator reinforced with rings with feet

The actuator was connected to the syringe using a connector and a blocker was affixed to the other end. The actuator was reinforced with rings with feet at valleys as shown in Fig 33. The responsiveness of the actuator was observed and recorded.

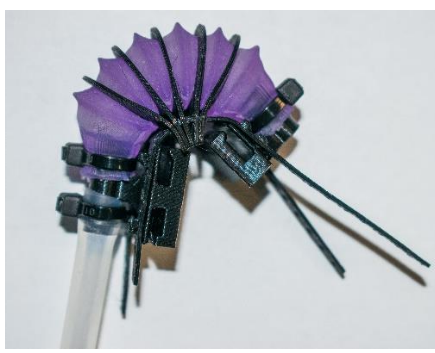

Figure 33 Actuator reinforced with rings having feet

3.6 Results

The following details given below were recorded during pressurizing he actuator using the syringe.

1. From the recorded data the actuator having no reinforcement shows the phenomenon of radial expansion.
2. Bulging can be seen in all three types of actuator types except for the actuator with the feet. The most bulging can be seen in the actuator without any reinforcements.
3. It is seen that the actuator reinforced with rings with feet has more curvature than other actuators because the bulging force is transformed into translating force.
4. It was noted that during negative pressure, the highest compression was seen in the actuator that has no reinforcement.
5. More linear translation was seen in the actuator with rings and the actuator with rings with feet when the limiting layer was removed, which can be used for thumb adduction and abduction.

Chapter 4

4 Conclusion and future work

4.1 Conclusion

This thesis proposes a simple wearable soft robotic glove and offers innovative solutions to address the complex manufacturing problem in the making of small soft actuators. The solutions that have been identified are how to use a disintegrable inner core, designing specific air channels to prevent air from being trapped inside the mold and carefully degassing the liquid silicone mixture without creating air bubbles. The reinforcement provided by the flexible TPU parts at the valleys of the bellows proved to affect the problems of bulging and is a solution to increase the range of motion of the actuator under pressure. Overall, this thesis has provided an innovative solution to design and manufacture small silicone actuators that provide positive-negative actuation. It has a suitable glove that can be manufactured for the presented actuator along with its reinforcement parts.

4.2 Future Works

In the future, the glove can be made even thinner, so that it is weightless. Since the actuator requires a threshold for wall thickness, the silicone rubber used to make the actuator can be changed to reduce the thickness of the wall of the actuator. More data needs to be collected on motion vs pressure. The frequency varying among various iterations of the actuator should be studied. The actuator can be made thick on one side and thin on the opposite side to translate the actuator in a particular direction when pressurized. A wearable pump with high-pressure input can be built so that the robotic glove is made portable.

References

[1] Van der Loos, H. M., Reinkensmeyer, D. J., & Guglielmelli, E. (2016b). Rehabilitation and Health Care Robotics. *Springer Handbook of Robotics*, 1685–1728. https://doi.org/10.1007/978-3-319-32552-1_64

[2] Kumar, A., Mundra, T. S., & Kumar, A. (2009). *Anatomy of Hand*. SpringerLink. pp 19 - 28

[3] C. Correia *et al*., "Improving Grasp Function After Spinal Cord Injury with a Soft Robotic Glove," in *IEEE Transactions on Neural Systems and Rehabilitation Engineering*, vol. 28, no. 6, pp. 1407-1415, June 2020, doi: 10.1109/TNSRE.2020.2988260.

[4] Shahid, T., Gouwanda, D., Nurzaman, S. G., & Gopalai, A. A. (2018). Moving toward Soft Robotics: A Decade Review of the Design of Hand Exoskeletons. *Biomimetics, 3*(3), 17. https://doi.org/10.3390/biomimetics3030017

[5] Chu, CY., Patterson, R.M. Soft robotic devices for hand rehabilitation and assistance: a narrative review. *J NeuroEngineering Rehabil* 15, 9 (2018). https://doi.org/10.1186/s12984-018-0350-6

[6] De Volder, M., & Reynaerts, D. (2010). Pneumatic and hydraulic microactuators: a review. *Journal of Micromechanics and Microengineering*, *20*(4), 043001. https://doi.org/10.1088/0960-1317/20/4/043001

[7] Polygerinos, P., Lyne, S., Zheng Wang, Nicolini, L. F., Mosadegh, B., Whitesides, G. M., & Walsh, C. J. (2013). Towards a soft pneumatic glove for hand rehabilitation. *2013 IEEE/RSJ International Conference on Intelligent Robots and Systems*. https://doi.org/10.1109/iros.2013.6696549

[8] Polygerinos, P., Wang, Z., Galloway, K. C., Wood, R. J., & Walsh, C. J. (2015). Soft robotic glove for combined assistance and at-home rehabilitation. *Robotics and Autonomous Systems*, *73*, 135–143. https://doi.org/10.1016/j.robot.2014.08.014

[9] D. Hu, J. Zhang, Y. Yang, Q. Li, D. Li, and J. Hong, "A Novel Soft Robotic Glove with Positive-negative Pneumatic Actuator for Hand Rehabilitation," *2020 IEEE/ASME International Conference on Advanced Intelligent Mechatronics (AIM)*, Boston, MA, USA, 2020, pp. 1840-1847, doi: 10.1109/AIM43001.2020.9158826.

[10] Y. Chen, S. Le, Q. C. Tan, O. Lau, F. Wan, and C. Song, "A lobster-inspired robotic glove for hand rehabilitation," 2017 IEEE International Conference on Robotics and Automation (ICRA), Singapore, 2017, pp. 4782-4787, doi: 10.1109/ICRA.2017.7989556

[11] *Leonardo Cappello, Kevin C. Galloway, Siddharth Sanan, Diana A. Wagner, Rachael Granberry, Sven Engelhardt, Florian L. Haufe, Jeffrey D. Peisner, and Conor J. Walsh* Exploiting Textile Mechanical Anisotropy for Fabric-Based Pneumatic Actuators Soft Robotics 2018 5:5, 662-674

[12] F. Lyu, M. Li, J. Guo, and S. Guo, "A New Fabrication Method for Soft Pneumatic Actuators based on Paraffin," *2022 IEEE International Conference on Mechatronics and Automation (ICMA)*, Guilin, Guangxi, China, 2022, pp. 340-344, doi: 10.1109/ICMA54519.2022.9856179.

[13] A Recipe for Soft Fluidic Elastomer Robots *Andrew D. Marchese, Robert K. Katzschmann, and Daniela Rus* Soft Robotics 2015 2:1, 7-25

[14] Patel, A. 2022, *Design and Fabrication of Accordion-Shaped Soft Actuators and Markerless Motion Evaluation*, New York University Tandon School of Engineering.

[15] Bhatt, N. 2022, *Bellow-Based Soft Actuators for Rehabilitation Purposes and Evaluation of Pneu-net Actuators*, New York University Tandon School of Engineering.